Janus gold nanoparticle with bicompartment polymer brushes templated by polymer single crystals

Bingbing Wang [a], Bin Dong [a], Bing Li [a], Bin Zhao [b], Christopher Y. Li [a,*]

[a] *Department of Materials Science and Engineering, Drexel University, Philadelphia, PA 19104, USA*
[b] *Department of Chemistry, University of Tennessee, Knoxville, TN 37996, USA*

ABSTRACT

Janus particles have attracted increasing attention from the communities of materials science, chemistry, physics and biology. While large size Janus particles are readily achieved, synthesizing Janus nanoparticles (JNP) with diameters smaller than ∼20 nm remains a challenging task. In this article, we report a systematic study on growing polymer brushes on polymer-single-crystal-immobilized 6 and 15 nm diameter gold nanoparticles (AuNPs) using atom transfer radical polymerization. JNPs with bicompartment polymer brushes, such as poly(ethylene oxide) (PEO)/poly(methyl methacrylate), PEO/poly(*tert*-butyl acrylate), and PEO/poly(acrylic acid), were synthesized. The grafting densities can be carefully controlled. The Janus feature of these particles was confirmed using both platinum nanoparticle decoration and UV/Vis spectroscopy analysis. The surface plasmon resonance absorbance of Janus particles exhibited a blue shift compared with that of symmetric AuNPs with either homopolymer or mixed polymer brushes. This work demonstrated that using polymer single crystal as the templates, small size (<20 nm diameter) JNPs having bicompartment polymer brushes can be readily obtained. The ability to tune grafting density and molecular weight of polymer brushes can lead to controlled particle amphiphilicity.

© 2010 Elsevier Ltd. All rights reserved.

1. Introduction

Janus particles are objects in micro or nanometer scale possessing a noncentrosymmetric structure, often with a single core that is surrounded by compartmentalized corona [1,2]. Since De Gennes first coined the name in 1991 [3], Janus particles have attracted increasing attention from the communities of materials science, chemistry, physics and biology [4]. Numerous Janus particles, with asymmetric geometry and/or surface chemistry, have been reported. Examples include dendrimers [5,6], block copolymer micelles [7–9], micrometer-size beads [10–17], nanofibers [18], and polymer microgels [19]. As a unique type of hybrid materials, Janus particles with a uniform metallic core, such as gold [20], have shown potential applications in the fields of photonics, optical biosensors, drug delivery, electronics, and Pickering emulsion [2,21–31]. Reported experimental methods to fabricate Janus particles include template-directed self-assembly [32,33], controlled phase separation [34–36], controlled surface nucleation [37–39], polymer salt quenching [40], and top-selective surface modification [41–43].

Among all these approaches, top-selective surface modification is the most popular one. During this process, particles are placed at the interface of two phases. One side of the particle is protected from modification, while the opposite side is modified chemically. As a result, Janus particles are obtained with different types of functional groups. Liquid−gas [44], liquid−liquid [19,45–47], and liquid−solid [17,48–51] interfaces have been investigated.

While Janus particles are readily achieved, synthesizing Janus nanoparticles (JNP) with diameters smaller than ∼20 nm remains a challenging task. There are only a few examples of small size JNPs in the literature. These include striped AuNPs formed by curvature-induced phase separation of small molar mass ligands [52] and asymmetrically functionalized nanoparticles synthesized using micro-magnetic particles, polystyrene (PS) beads, or silanized glass as the templates [52–54]. JNPs with phase separated polymer brushes were reported in a thiol-ended PS (PS−SH)/thiol-ended poly(2-vinylpyridine) (P2VP−SH)/gold nanoparticle (AuNP) system. AuNPs grafted with PS−SH and P2VP−SH with different molar ratios were blended into a lamellae-forming PS-*b*-P2VP block copolymer. The location of the PS/P2VP-coated nanoparticles was found to be a function of the PS volume fraction: they are located in the PS domain, PS/P2VP interface, and P2VP domain when $F_{PS} > 0.9$, $0.1 < F_{PS} < 0.9$ and $F_{PS} < 0.1$, respectively. The wide F_{PS} window of

which the AuNPs were located at the PS/P2VP interface was attributed to the formation of Janus AuNPs with PS/P2VP brushes [53]. Using silica microsphere as the mask, Hatton et al. synthesized Janus magnetic nanoparticles (Fe_3O_4) with poly(acrylic acid) (PAA)/ sodium polystyrene sulfonate and PAA/poly(N,N-dimethylami-noethyl methacrylate) brushes. Temperature responsive assembly behavior was observed [54].

Polymer single crystals can also be used as solid substrates for JNP synthesis [55−57]. Polymer single crystals are often considered as quasi-two-dimensional lamellae, which are formed by folding polymer chains back and forth; the chains are perpendicular or oblique to the lamellar surface [58−61]. Interaction between this unique material and nanoparticles has recently been explored [59,62,63]. As the chain ends are different from the rest of the polymer backbone, given the right crystallization condition, they are excluded onto the surface of the lamellar crystals. Judiciously selected nanoparticles can then be bound onto the single crystal surface via chemisorptions [59,64,65]. If we consider a polymer lamella as a thin sheet of paper, lamella with functional groups on the surface can then be regarded as a nanoscale sticky tape, which can immobilize different nanoparticles [59,66,67]. Recently, it has been demonstrated that pre-formed AuNPs can be immobilized onto the surface of thiol-ended poly(ethylene oxide) (PEO−SH) single crystals via coupling with the polymer chain ends (grafting-to) [55]. In this way, polymer single crystals are used as the solid mask for JNP synthesis. The opposite side of the nanoparticles can be further functionalized with different functional groups [57]. In this article, we report a systematic study on growing polymer brushes with different molecular weights and hydrophobicity on polymer-single-crystal-immobilized AuNPs using surface-initiated atom transfer radical polymerization (ATRP) [68,69]. JNPs with bicompartment polymer brushes and different particle sizes were synthesized. The grafting densities of each type of brushes were carefully controlled. Symmetric AuNPs with homo and mixed polymer brushes were also synthesized and their surface plasmon resonance (SPR) absorption was compared with that of the JNP. This work demonstrates that using polymer single crystals as the templates, JNPs with bicompartment polymer brushes can be readily synthesized.

2. Experimental

2.1. Materials

PEO−SH ($M_n \sim$ 5 K g mol^{-1}) was purchased from Polymer Source Inc. Methyl methacrylate (MMA, 99%), *tert*-butyl acrylate (*t*BA, 98%+), and toluene (98%+) were purchased from Aldrich and redistilled under vacuum. Gold (III) chloride (99%), tetrabu-tylammonium borohydride (TBAB, 98%), didodecyldimethy-lammonium bromide (DDAB, 98%), trifluoroacetic acid (99.0%+), 11-mercapto-1-undecanol (97%), 2-bromoisobutyryl bromide (98%), pyridine (anhydrous, 99.8%), tri(2-aminoethyl)amine (98.0%+), formic acid (∼98%), formaldehyde solution (37 wt% in H_2O), tributylphosphine, chloroplatinic acid hydrate (99.9%), hydrazine (anhydrous, 98%), copper (I) bromide (98%), potassium hydroxide (85%+), and aluminum oxide (activated, neutral, for column chromatography, 50−200 μm) were purchased from Aldrich and used as received. Sodium hydroxide was obtained from Fisher and used as received. AuNPs (6 nm in diameter) were synthesized according to literature [70]. Me$_6$TREN were synthe-sized as reported [57]. All other chemical reagents including acetone, diethyl ether, chloroform, toluene, and methanol were purchased from either Aldrich or Fisher and were used without further purification.

2.2. Synthesis of Janus AuNPs

Janus AuNPs are denoted as A_m-Au_X-B_n. A and B stand for the ligand/polymer grafted on AuNPs; m and n (if used) stand for the degree of polymerization of the corresponding polymer brushes. X (if used) denotes the AuNP diameter (in nm).

2.2.1. Synthesis of initiator − and PEO$_{114}$-modified Janus AuNPs (PEO$_{114}$-Au-I)
##### 2.2.1.1. Growth of PEO$_{114}$ single crystals.
PEO/pentyl acetate solution (320 g, 0.06 wt%) was heated to 60 °C for 10 min. The solution was cooled to −10 °C and kept at this temperature overnight. The solution was then heated to 45 °C for 10 min to form crystal seeds. The final crystallization was conducted at 25 °C for 24 h. Free PEO was removed by centrifugation. The morphology of PEO single crystals was studied using TEM and AFM.

Janus AuNPs (6 nm in diameter) modified with initiator and PEO (PEO$_{114}$-Au$_6$-I). A solution of AuNPs in toluene (133 g, 0.2 wt %) was added dropwise into the suspension of PEO$_{114}$ single crystals in pentyl acetate (665 g, 0.03 wt%) under magnetic stir-ring. The solution was stirred at room temperature for 24 h. Multiple centrifugations were performed to remove free AuNPs. The AuNP-decorated PEO single crystals were re-dispersed in 200 g pentyl acetate. A solution of initiator 11-mercaptoundecyl 2-bromo-2-methylpropionate **1** (the structure is shown in Scheme 1) in pentyl acetate was added and the final concentra-tion of **1** in the single crystal suspension was kept at 1 wt%. The mixture was stirred at room temperature for 24 h. Multiple centrifugations were applied to remove the free initiator. Complete removal of the free initiator was confirmed by ^{1}H NMR spectroscopy analysis.

2.2.1.2. Janus AuNPs (15 nm in diameter) modified with initiator **1** and PEO (PEO$_{114}$-Au$_{15}$-I).
Initiator **1** − modified symmetric AuNPs with the diameter of 15 nm (I-Au$_{15}$) (75 mg) was dispersed in 10 ml chloroform. The solution was slowly added into the PEO$_{114}$ single crystal suspension in pentyl acetate (50 g, 0.2 wt%). After 3 h, the single crystals were separated from the solution by centrifugation. Additional 75 mg I-Au$_{15}$ in chloroform was added and the reaction was conducted for 3 h. The immobilization/centrifugation process was repeated until the free solution after centrifugation showed a red color, which indicated the saturation of AuNPs on the surface of single crystals.

2.2.2. Synthesis of PMMA- and PEO-modified Janus AuNPs with the diameter of 6 nm (PEO$_{114}$-Au$_6$-PMMA)
CuBr (12.0 mg, 0.0840 mmol), PEO$_{114}$-Au$_6$-I (single crystal form) in 20 g pentyl acetate (0.1 wt%), initiator **1** (30 mg, 0.085 mmol) in 1 ml toluene [71], Me$_6$TREN (19.0 mg, 0.0852 mmol) in 1 ml toluene, and MMA (2.040 g, 20.40 mmol) in 2 ml toluene were added into a Schlenk tube. Three cycles of freeze-pump-thaw were performed to degas the reaction mixture. The polymerization was conducted at room tempera-ture. After 24 h, the polymerization was stopped by opening the tube to air. The reaction mixture was centrifuged and the iso-lated PEO single crystals with the immobilized AuNPs were washed three times with a mixed solvent of pentyl acetate/ toluene (5/1, v/v). The product was dissolved/dispersed in chlo-roform and the mixture was then precipitated in methanol to remove free PEO. Fractionated precipitation was conducted to remove free PMMA formed from the sacrificial initiator using acetone and methanol as solvent and non-solvent, respectively. The final precipitate was collected and dried in vacuum at 35 °C for 24 h. PEO$_{114}$-Au$_6$-PMMA was characterized using ^{1}H NMR, GPC, TGA and TEM.
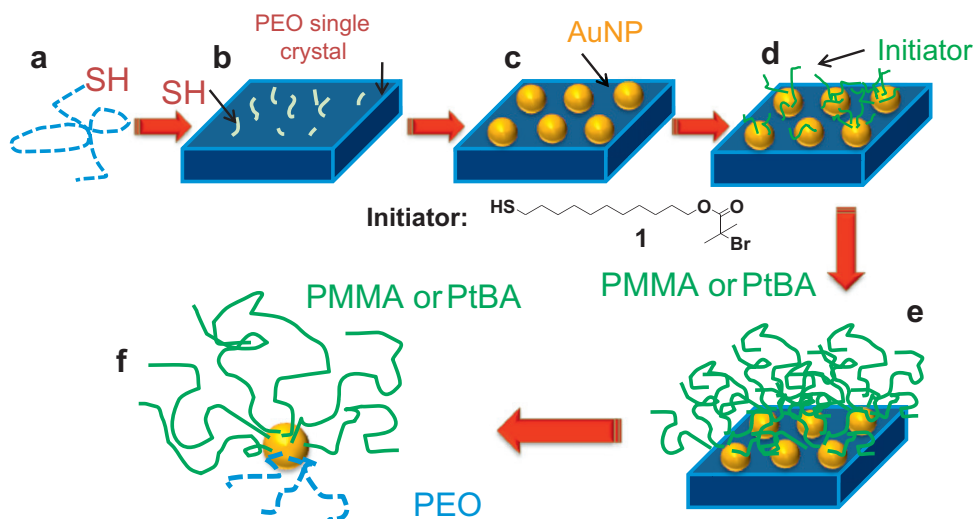
Scheme 1. Schematic illustration of polymer-functionalized Janus AuNPs by combining "grafting-to" and "grafting-from" methods. (a) PEO–SH, (b) PEO–SH single crystals with HS groups on the Surface, (c) AuNPs immobilized on PEO–SH single crystals, (d) Initiators coated on the top surface of the immobilized AuNPs, (e) Growth of polymer brushes on polymer-single-crystal-immobilized AuNPs, and (f) Dissolution of the polymer single crystals leading to the formation of Janus AuNPs with bicompartment polymer brushes.

2.2.3. Synthesis of poly(tert-butyl acrylate) (PtBA)- and PAA-modified Janus AuNPs with the diameter of 15 nm (PEO$_{114}$-Au$_{15}$-PtBA)

CuBr (13 mg, 0.091 mmol), initiator **1** (70 mg, 0.20 mmol) in 1 ml toluene, PEO$_{114}$-Au$_{15}$-I in 20 g pentyl acetate (0.1 wt%), Me$_6$TREN (22.3 mg, 0.100 mmol) in 1 ml toluene, and *tert*-butyl acrylate (2.38 g, 18.6 mmol) in 2 ml toluene were added into a Schlenk tube. The mixture was degassed by three freeze-pump-thaw cycles, and the polymerization was carried out at room temperature. After 24 h, the reaction was stopped by opening the tube to air. The PEO single crystals with the immobilized AuNPs and PtBA brushes were isolated by centrifugation and washed three times with a mixed solvent of pentyl acetate/toluene (5/1, v/v) to remove the free PtBA and ligand. Acetone was used to dissolve the mixture of Janus AuNPs and free PEO. Diethyl ether was slowly added into the solution until the formation of a dark-red precipitate. Janus AuNPs modified with PEO and PtBA precipitated first because of the highly concentrated polymers on the surface of AuNPs. After separating the precipitate from the solution, it was collected and redissolved in acetone. This process was performed at least seven times to remove the free polymer from the Janus AuNPs modified with PEO and PtBA. The final product was dried under vacuum at 35 °C for 24 h. Janus PEO$_{114}$-Au$_{15}$-PAA was formed by hydrolysis of PEO$_{114}$-Au$_{15}$-PtBA. Platinum nanoparticles (PtNPs) were synthesized in situ on PAA bushes. These two processes were conducted following the procedure reported previously [57].

2.3. Synthesis of symmetrically functionalized AuNPs

Symmetrically functionalized AuNPs are denoted as A$_m$-Au$_X$ and A$_m$/B$_n$-Au$_X$. A and B stand for the ligand/polymer grafted on AuNPs; m and n (if used) stand for the degree of polymerization of the corresponding polymer brushes. X (if used) denotes the AuNP diameter (in nm). A$_m$-Au$_X$ indicates that the particle is grafted with a single type of ligand/polymer brush, whereas A$_m$/B$_n$-Au$_X$ stands for mixed-ligand/brush-modified AuNPs.

2.3.1. Synthesis of initiator-modified symmetric AuNPs (I-Au)

Initiator **1** (330 mg, 1.05 mmol) in 2 ml toluene was slowly added into 150 g AuNP solution in toluene (~6 nm in diameter, 0.2 wt%). The mixture was stirred at room temperature overnight under nitrogen. 300 ml methanol was slowly added into the reaction mixture until the appearance of precipitation. The mixture was separated by centrifugation. The precipitate was washed with methanol three times in order to remove the free initiator. The resultant initiator-modified AuNPs with the diameter of 6 nm (I-Au$_6$) were collected and dried at room temperature under vacuum for 24 h. Initiator-modified AuNPs with the diameter of 15 nm (I-Au$_{15}$) were synthesized using the same procedure with the molar ratio between gold atom and initiator to be **1**. ^{1}H NMR spectroscopy and TGA were used to characterize the initiator-modified AuNPs.

2.3.2. Synthesis of poly(methyl methacrylate)-modified symmetric AuNPs (PMMA-Au$_6$)

CuBr (8.00 mg, 0.056 mmol), I-Au$_6$ (36.0 mg) in 2 ml toluene, Me$_6$TREN (13 mg, 0.058 mmol) in 2 ml toluene, initiator **1** (20 mg, 0.057 mmol) in 2 ml toluene, MMA (1.362 g, 13.62 mmol) in 4 ml toluene were added in a Schlenk tube. Three cycles of freeze-pump-thaw were then performed. Polymerization was conducted at room temperature. After 24 h, polymerization was stopped by opening the tube to air. The reaction mixture was precipitated into methanol. The product was dissolved in chloroform and then precipitated in methanol three times. Fractionated precipitation was performed to remove free PMMA by using acetone and methanol as the solvent and non-solvent, respectively. The final precipitate was collected and dried under vacuum at 35 °C for 24 h.

2.3.3. Synthesis of PEO$_{114}$- and initiator-modified symmetric AuNPs (PEO$_{114}$/I-Au$_6$)

I-Au$_6$ (23.1 mg) was dissolved in 30 ml dichloromethane. PEO–SH (PEO$_{114}$, 164 mg) was added and the mixture was stirred at room temperature for 5 days under nitrogen. Fractionated precipitation using acetone/diethyl ether as solvent/non-solvent was performed multiple times to remove free PEO. The final product was collected and dried under vacuum at 35 °C for 24 h.

2.3.4. Synthesis of mixed-brush symmetric AuNPs (PEO$_{114}$/PMMA-Au$_6$)

CuBr (8.0 mg, 0.056 mmol), PEO$_{114}$/I-Au$_6$ (70 mg), Me$_6$TREN (13.0 mg, 0.0580 mmol), initiator **1** (20 mg, 0.0570 mmol), MMA (1.362 g, 13.62 mmol) in 10 ml toluene were added in a Schlenk

tube. Three cycles of freeze-pump-thaw were then performed. Polymerization was conducted at room temperature. After 24 h, polymerization was stopped by opening the tube to air. The product was dissolved in chloroform and then precipitated in methanol three times. Fractionated precipitation was performed. The final precipitate was collected and was dried in vacuum at 35 °C for 24 h.

2.4. Measurement

^{1}H NMR spectra were recorded on either a UnityInova 500 MHz or a 300 MHz spectrometer using CDCl$_3$ as the solvent and tetramethylsilane (TMS) as the internal standard. Transmission electron microscopy (TEM) was carried out using a JEOL JEM2100 TEM operated at an acceleration voltage of 200 kV. To prepare the TEM sample, one drop of single crystal or nanoparticle suspension was cast on a carbon-coated nickel grid. After solvent evaporation, the sample was used for TEM observation without further treatment. UV–Vis spectra were collected using an Ocean Optics USB4000 Miniature Fiber Optic Spectrometer at room temperature. Infrared spectra were recorded using a Digilab, UMA 600 FTIR spectrometer with KBr pellets in transmission mode. A sample solution (1 g, 0.1 wt%) was drop cast on the surface of KBr pellets and was dried under vacuum for 24 h. Before FTIR test, the KBr pellets were dried again using an infrared lamp for at least 10 min. Gel permeation chromatography (GPC) was carried out using a Waters GPC system with a 1525 binary HPLC pump, a Waters 2414 refractive index detector, and one Styragel® HR 4 THF (300 × 7.8 mm) column. The data were processed using Breeze software. THF was used as the carrier solvent at a flow rate of 1.0 ml/min. Standard monodispersed polystyrenes were used for calibration. All the GPC

experiments were run at 40 °C. Thermogravimetric analysis (TGA) was conducted using a Perkin–Elmer TGA-7. The sample was heated in nitrogen from 50 °C to 800 °C with a heating rate of 10 °C/min. Before analysis, the samples were dried under vacuum at 50 °C for 24 h.

3. Results and discussion

3.1. Synthesis of PEO- and initiator-modified Janus AuNPs

Synthesis of PEO- and initiator-modified Janus AuNPs was achieved using PEO single crystals as the template. As shown in Scheme 1, we first grew PEO–SH single crystals with the thiol groups exposed on the surface. For 6 nm AuNPs, AuNPs modified with ammonium salt were mixed with the PEO–SH single crystal suspension in a mixed solvent of pentyl acetate/toluene (5/1, v/v). After 24 h of reaction, AuNPs were immobilized on the surface of PEO single crystals (Scheme 1c, grafting-to). In doing so, the "bottom part" of AuNP was coupled with the surface of single crystals and the AuNP symmetry was broken. The opposite hemisphere of the AuNP was then available for chemical modification with thiol-ended ligands, such as the ATRP initiator **1** (Scheme 1), via ligand exchange reactions. The PEO- and initiator **1**-modified Janus AuNPs (PEO$_{114}$-Au$_6$-I) was obtained by mixing the AuNP-decorated PEO single crystals with **1** in pentyl acetate (1 wt%) for 24 h (Scheme 1d). Free initiator, other ligands as well as free AuNPs were easily removed by multiple centrifugations. Fig. 1a–c shows TEM images of the ammonium salts (TBAB/DDAB, 1:2 M ratio)-protected AuNPs and PEO single crystals with the immobilized AuNPs. Synthesis of PEO$_{114}$-Au$_{15}$-I was achieved by a different method, because the ammonium salts-protected large diameter
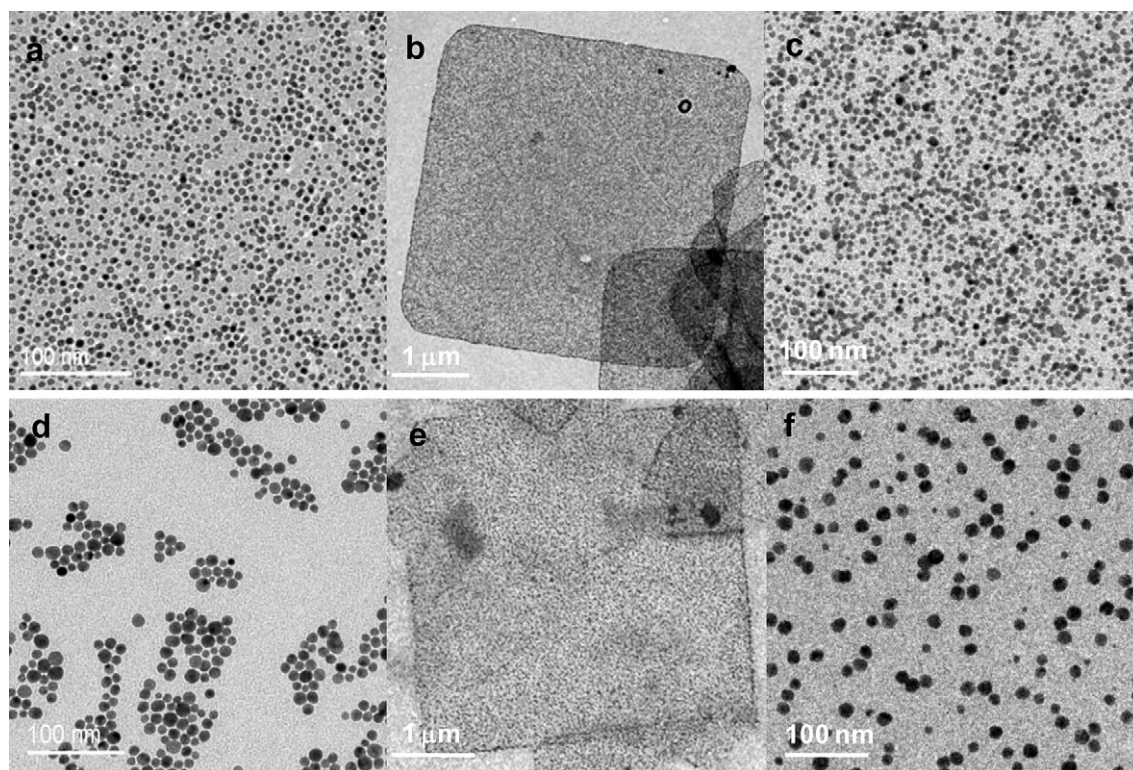
Fig. 1. TEM images of immobilization of AuNPs with the diameter of 6 (a–c) and 15 (d–f) nm onto PEO–SH single crystals. (a) Ammonium salts-protected 6 nm AuNPs, (d) initiator-modified 15 nm AuNPs. (b) and (e) show that these nanoparticles were immobilized on squared-shaped PEO single crystals. (c) and (f) show the enlarged areas of (b) and (e), respectively.

AuNPs were unstable in the mixed solvent of toluene and pentyl acetate. To avoid aggregation, 15 nm AuNPs were first modified with **1** to form Au$_{15}$-I, after which the AuNPs were dissolved in chloroform (Fig. 1d), and were mixed with PEO single crystals using chloroform/pentyl acetate (1/5, v/v) as the solvent. TEM images confirmed that these AuNPs were immobilized on the surface of PEO single crystals (Fig. 1e and f). The successful coupling between Au$_{15}$ and PEO single crystals is because of the place exchange reaction between initiator **1** and surface thiol groups of PEO$_{114}$ single crystals [72]. Although similar thiol-Au bonding occurs for both **1**/AuNP and PEO–SH/AuNP, because of the plane nature of the single crystal surface and the relatively high end group density on the crystal surface, each AuNP can form multiple bonds with the crystal. Therefore, once one initiator **1**/AuNP bond exchanges with one PEO–SH/AuNP, it facilitates the bonding process between adjacent PEO–HS and the AuNP, pushing the exchange reaction towards the formation of PEO–HS/AuNPs. As shown in Fig. 1, the density of AuNPs on the surface of single crystals varies with the nanoparticle size, which might be caused by the different efficiency of the ligand exchange reactions for these two types of nanoparticles: PEO–SH replaced ammonium salts in the 6 nm AuNP system, while it exchanged initiator **1** in the 15 nm AuNP case. The former reaction is more readily to occur due to the relatively weak gold–ammonium interaction as opposed to the Au-thiol bond.

3.2. Synthesis of Janus AuNPs with bicompartment brushes

Janus AuNPs with PEO/PMMA and PEO/PtBA bicompartment brushes have been synthesized from PEO-Au-I using ATRP. In order to maintain the asymmetric properties, several conditions were chosen: 1) Pentyl acetate was used as the solvent for the polymerization. Because PEO single crystals were formed in pentyl acetate, and were used as the template for brush synthesis, a polymerization in the same solvent will less likely break/dissolve the single crystals. 2) All of the surface-initiated polymerizations were performed at room temperature in order to avoid the dissociation of thiol-gold bonds. 3) Me$_6$TREN-CuBr catalyst system was used since it had less influence on the dissociation of thiol-functionalized ligands from gold surface during the polymerization [73,74]. PMMA was grown from PEO$_{114}$-Au$_6$-I and PtBA was grown from PEO$_{114}$-Au$_{15}$-I. Fractionated precipitation was then used to purify the Janus AuNPs. Removal of the free polymers was confirmed by GPC experiments (Fig. S1 in Supporting Information).

3.3. Characterization of AuNPs and grafting density study

3.3.1. Initiator-modified symmetric AuNPs (I-Au)

Fig. 2a shows the ^{1}H NMR spectra of initiator (spectrum I) and I-Au (spectrum II for 6 nm AuNPs and III for 15 nm AuNPs) in CDCl$_3$. The covalent bonding of the initiator to the surface of AuNPs leads to the broadening of peaks (4), (5) and (6) in spectrum II and III. For spectrum III, a peak at $\delta \sim 2.67$ ppm is observed, which might arise from the loosely attached surface ligands [75]. From FTIR spectra (Fig. 2b), characteristic signals from the surface of AuNPs, such as C=O stretching around 1732 cm^{-1}, match well with those from the initiator (spectrum I in Fig. 2b). The C–H stretching from –CH$_2$– shifted from 2854 cm^{-1} and 2927 cm^{-1} for free initiator to around 2850 and 2915 cm^{-1} for I-Au, which indicated an increasing ordering of alkyl chains for initiator after binding to the surface of AuNPs [73]. In order to study the initiator contents, TGA experiments were performed. The weight percentage of nanoparticles was obtained by heating the sample from 50 °C to 700 °C under nitrogen with the heating rate of 10 °C/min. The nanoparticle contents for I-Au$_6$ and I-Au$_{15}$ were 85 and 87%, respectively. The initiator densities on 6 and 15 nm AuNPs were calculated to be 5.8 and 9.42 initiators/nm^2, respectively, which match well with the previously reported values. Note that the surface areal initiator density for I-Au$_{15}$ is relatively high, which might be caused by the loosely attached ligand on the surface as shown in Fig. 2a (spectrum III).

3.3.2. PEO- and initiator-modified Janus AuNPs (PEO$_{114}$-Au-I) and symmetric AuNPs (PEO$_{114}$/I-Au)

Fig. 3 shows the ^{1}H NMR spectra of AuNPs modified with PEO and initiator **1** including Janus and symmetric AuNPs. The characteristic peaks from the initiator at $\delta \sim 1.9$ ppm (–CH$_3$) and from PEO at $\delta \sim 3.65$ ppm (–CH$_2$O–) can be seen. All of the –CH$_2$– (6) from the backbone of the initiator on the surface of AuNPs gave a broad signal of $\delta \sim 1.2$–1.4 ppm, which matched well with that from the pure initiator (Fig. 3a). However, only one broad peak was observed in Fig. 3b and c at $\delta \sim 1.5$–1.7 ppm, which corresponded to –CH$_2$– (4) and (5). This might be attributed to the reduced mobility of the molecules caused by the bonding of the initiator to the surface of AuNPs.

The synthesis of symmetric PEO$_{114}$/I-Au6 was achieved by mixing initiator-modified AuNPs with PEO–SH in solution and allowing the ligand exchange reaction between PEO–SH and **1**.
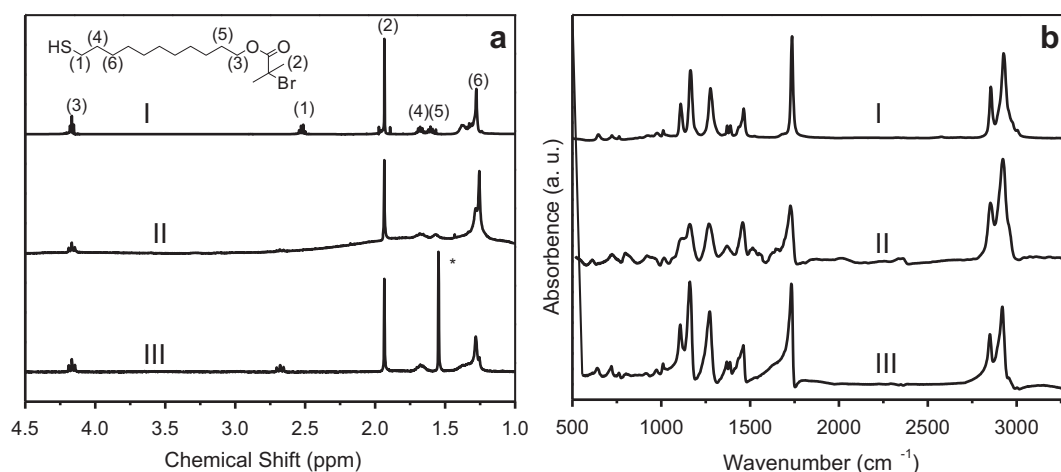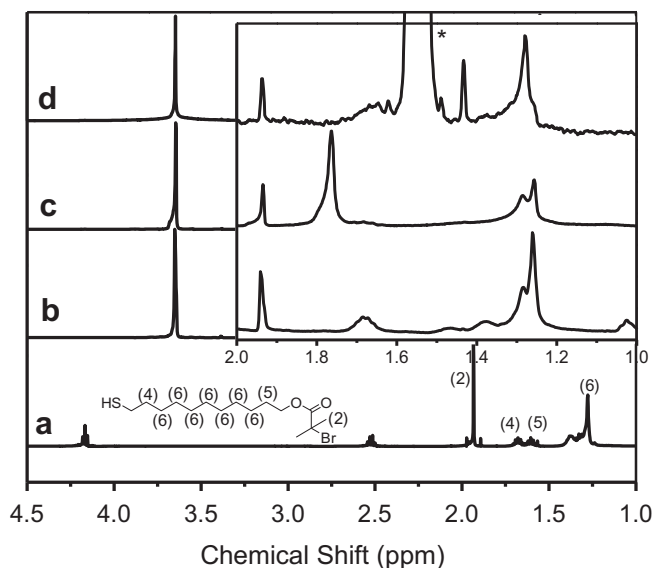

Fig. 2. ^{1}H NMR (a) and FTIR (b) spectra of initiator (I), initiator-modified AuNPs with the diameters of 6 nm (II) and 15 nm (III) (*: solvent).

Fig. 3. ^{1}H NMR spectra of initiator (a), PEO- and initiator-modified Janus AuNPs PEO$_{114}$-Au$_6$-I (b), PEO$_{114}$-Au$_{15}$-I (c), and PEO- and initiator-modified symmetric AuNPs PEO$_{114}$/I-Au$_6$ (d). The inset shows the enlarged spectra from $\delta \sim 1.0$–2.0 ppm (*: solvent).

Fig. 3d shows the ^{1}H NMR spectrum of such symmetric particles. The grafting density was calculated using ^{1}H NMR (Fig. 3d) and TGA results as shown in Table 1. The total surface areal chain density decreased from 5.8 chains/nm^2 for Au$_6$-I to 2.0 chains/nm^2 for PEO$_{114}$/I-Au$_6$, and the number of surface initiator per particle decreased from 656 for Au$_6$-I to 151 for PEO$_{114}$/I-Au$_6$.

3.3.3. PEO- and PMMA-modified symmetric and Janus AuNPs (PEO$_{114}$/PMMA-Au$_6$, PEO$_{114}$-Au$_6$-PMMA)

After the surface modification with polymer brushes, both symmetric and Janus AuNPs can be dispersed in organic solvents such as acetone. Fig. 4 shows the TEM images of solution cast nanoparticles; no particle aggregation was observed. For symmetric AuNPs modified with mixed brushes of PEO and PMMA, both PEO ($\delta \sim 3.65$ ppm) and PMMA ($\delta \sim 3.61$, 1.82, 1.03, and 0.84 ppm) signals were observed in the ^{1}H NMR spectrum (Fig. 5a). The molecular weight of PMMA was found to be 15.2 K g/mol measured by GPC. The molar ratio of PEO and PMMA was calculated by comparing $-CH_2O-$ of PEO ($\delta \sim 3.65$ ppm) and $-OCH_3$ of PMMA ($\delta \sim 3.61$ ppm) peaks. For PEO- and PMMA-modified Janus AuNPs, similar results were obtained from ^{1}H NMR spectrum (Fig. 5).

Table 1
Surface characteristics of symmetric AuNPs.

|	$M_{n,I}$[a]	$M_{n,PEO}$[a] (K)	$M_{n,PMMA}$[a] (K)	N_I[b]	N_{PEO}[b]	N_{PMMA}[b]	σ[c]
I-Au	353			656	–		5.8
PEO$_{114}$/I-Au$_6$	353	5		151	77		2.0
PEO$_{114}$/ PMMA$_{152}$-Au$_6$	–	5	15.2		71	63	1.2
PMMA$_{130}$-Au$_6$	–	–	13	–	–	93	0.82

[a] Molecular weight of surface ligand/polymer (g/mol).
[b] Average chain number per AuNP.
[c] Overall grafting density (chains/nm^2).

Moreover, with increasing PMMA molecular weight from 11.8 K, to 20.8 K g/mol (Fig. 5c and d), the peak intensity at $\delta \sim 3.61$ ppm corresponding to PMMA increased gradually. It should be noted that the polydispersity indices (PDI) of these PMMA brushes (obtained by measuring free PMMA chains) are around 1.2, smaller than that of the previously reported 1.47 for PMMA brushes synthesized without using a sacrificial initiator [57]. The organic contents of these polymer-modified AuNPs were obtained from TGA (Fig. 6). Combining TGA, NMR and GPC results, the surface grafting densities of both symmetrical and Janus AuNPs were calculated and are shown in Tables 1 and 2. Of interest is that for symmetric AuNPs modified with PEO and PMMA, the PEO grafting density did not change significantly before and after polymerization, which indicates that the reaction and purification processes had a negligible effect on the stability of the Au-thiol bond. As shown in Table 1, there are less PMMA chains than that of the initiator, which indicates that only a fraction of (~ 0.42) the initiator initiated the chain growth.

For Janus AuNPs with bicompartment PEO and PMMA brushes, the grafting densities of PEO and PMMA brushes were investigated. The average grafting density (including both PEO and PMMA) decreased from 0.87 chains/nm^2 for PEO$_{114}$-Au$_6$-PMMA$_{118}$ to 0.52 chains/nm^2 for PEO$_{114}$-Au$_6$-PMMA$_{208}$. The number of PEO chains on each AuNP is around 30 for all three samples. This can be attributed to that the PEO chains were attached to the AuNPs during the immobilization process of AuNPs on PEO single crystals. Therefore, the PEO chain number was determined by the coupling reaction occurred at the interface of single crystals and nanoparticles. The subsequent surface-initiated polymerization did not affect the stability of the thiol-gold bond; hence the number of PEO on the AuNPs did not change before and after the polymerization. Also of interest is that the number of PEO chains per AuNP is smaller than that of the previously reported Janus AuNPs using 2 K g/mol PEO as the single crystal substrate (70 chains/particle in the later case) [57].
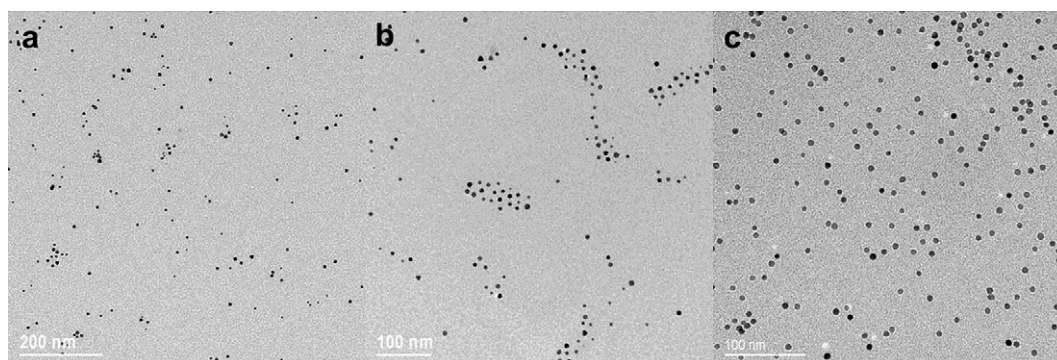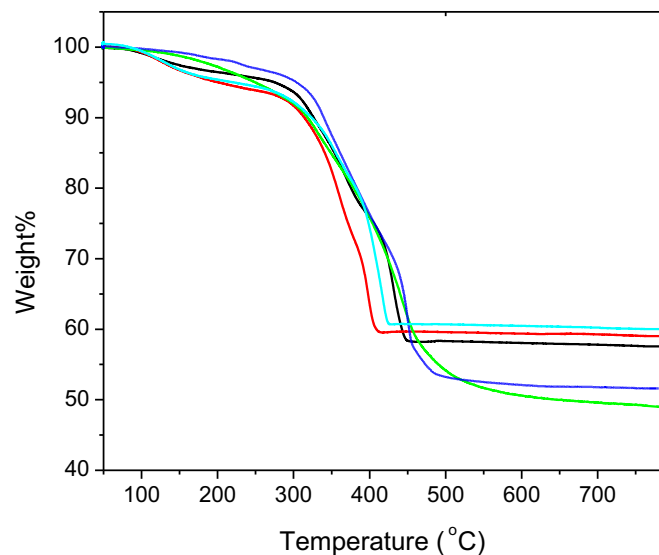

Fig. 4. TEM images of symmetric AuNPs PEO$_{114}$/I-Au$_6$ (a), PEO$_{114}$/PMMA$_{152}$-Au$_6$ (b), and Janus PEO$_{114}$-Au$_6$-PMMA$_{208}$ (c), cast from acetone solutions.
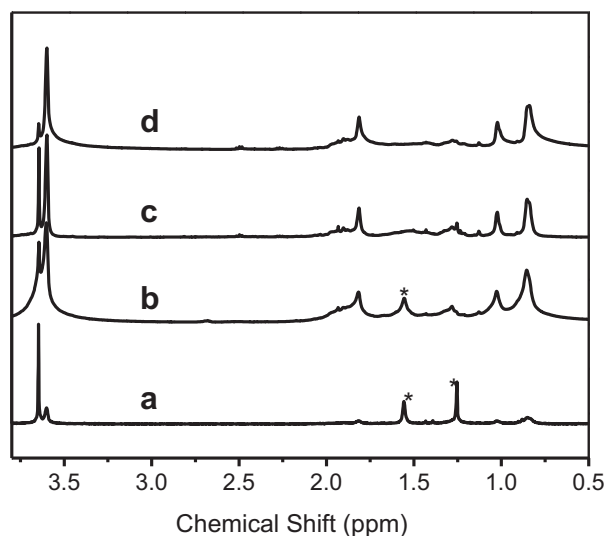
Fig. 5. ^{1}H NMR spectra of PEO- and PMMA-modified symmetric AuNPs PEO$_{114}$/PMMA$_{152}$-Au$_6$ (a), and Janus AuNPs PEO$_{114}$-Au$_6$-PMMA$_{118}$ (b), PEO$_{114}$-Au$_6$-PMMA$_{138}$ (c), and PEO$_{114}$-Au$_6$-PMMA$_{208}$ (d) (*: solvents).

Fig. 6. TGA of PEO- and PMMA-modified AuNPs from bottom to top: symmetric AuNPs PEO$_{114}$/PMMA$_{152}$-Au$_6$, symmetric PMMA$_{130}$-Au$_6$, Janus AuNPs PEO$_{114}$-Au$_6$-PMMA$_{118}$, PEO$_{114}$-Au$_6$-PMMA$_{138}$, and PEO$_{114}$-Au$_6$-PMMA$_{208}$.

This can be explained by the unique integer chain folding of polymers with low molecular weights. For 2 K g/mol PEO single crystals, as we reported previously, the lamellar thickness is ∼ 12 nm and the polymer formed extended chain single crystals. In the present 5 K g/mol PEO case, AFM (Fig. 7) showed that the lamellar thickness was ∼ 16 nm, indicating a once-fold crystal. Because in both 2 K and 5 K PEO cases, there is one thiol group per chain, changing from an extended chain conformation to a once-fold conformation reduced the surface areal density of thiol groups by a factor of 2. As a result, the average number of PEO chains attached to the surface of AuNPs approximately dropped by a factor of 2 (30 vs. 70 chains/particle). This observation also suggests that semi-quantitative control of grafting density of polymer chains by controlling the polymer molecular weight is feasible.

Also of interest is that with increasing the molecular weight of PMMA, the number of PMMA chains per AuNP decreased from 68 to 26. The decrease of PMMA grafting density on the surface of AuNPs may be attributed to the steric hindrance imposed by polymer brushes, and/or possible desorption of polymer chains during polymerization [76].

3.4. Platinum nanoparticle (PtNP) decorated Janus AuNPs (PEO$_{114}$-Au$_{15}$-PAA$_{109}$-PtNPs)

In order to demonstrate the Janus nature of the nanoparticles, PtNP-decoration method was used. To facilitate the formation of

nanoparticle in the brushes synthesized by surface-initiated ATRP, PtBA instead of PMMA was grown from the Janus AuNP surface and subsequently hydrolyzed to PAA. PtBA molecular weight was measured to be 13.9 K g/mol with a PDI of 1.1. The resultant PEO- and PtBA-modified Janus AuNPs were spread on water surface, picked up using a carbon-coated grid, and were subjected to TEM observation. Fig. 8a shows a TEM image of PEO$_{114}$-Au$_{15}$-PtBA$_{109}$ dispersed on water; no particle aggregation was observed. The relatively large inter-particle distance compared with Fig. 1d is due to the grafted polymer brushes [77]. PtBA brushes were then hydrolyzed to yield PAA. The formation of PAA on the surface of Janus AuNPs was confirmed by ^{1}H NMR (Fig. S2). PtNPs were then synthesized using the in-situ reduction method following the reported procedure [57]. In brief, chloroplatinic acid hydrate solution in methanol was added to PAA-modified AuNP solution in methanol. Aqueous solution of hydrazine was added into the mixture solution with vigorous stirring and PtNPs were then formed. Fig. 8b and c clearly shows that part of the AuNP surface was covered by small PtNPs with the diameter around ∼ 2 nm. The "empty" area on the AuNPs surface is attributed to the coverage of PEO chains, which was not able to absorb platinum ions for PtNP formation [57]. Of interest is that in Fig. 8c, the relatively higher platinum salt concentration (five times higher as compared to that of Fig. 8b) led to the formation of dendrite-like PtNPs on the AuNP surface. Yet, the PEO region remained intact from PtNPs, further confirming the Janus nature of the AuNPs.

Table 2
Surface characteristics of Janus AuNPs with bicompartment brushes.

	M$_{nPEO}$[a]	M$_{nPMMA}$[a]	PDI[b]	Au %[c]	R$_1$[d]	R$_2$[e]	N$_{PEO}$[f]	N$_{PMMA}$[f]	σ[g]
PEO$_{114}$-Au$_6$-PMMA$_{118}$	5	11.8	1.25	58	1/2.29	1/5.4	30	68	0.87
PEO$_{114}$-Au$_6$-PMMA$_{138}$	5	13.8	1.24	59	1/2.56	1/7.1	27	56	0.73
PEO$_{114}$-Au$_6$-PMMA$_{208}$	5	20.8	1.25	61	1/0.76	1/3.2	32	26	0.52

[a] Molecular weight of polymer brushes (K g/mol).
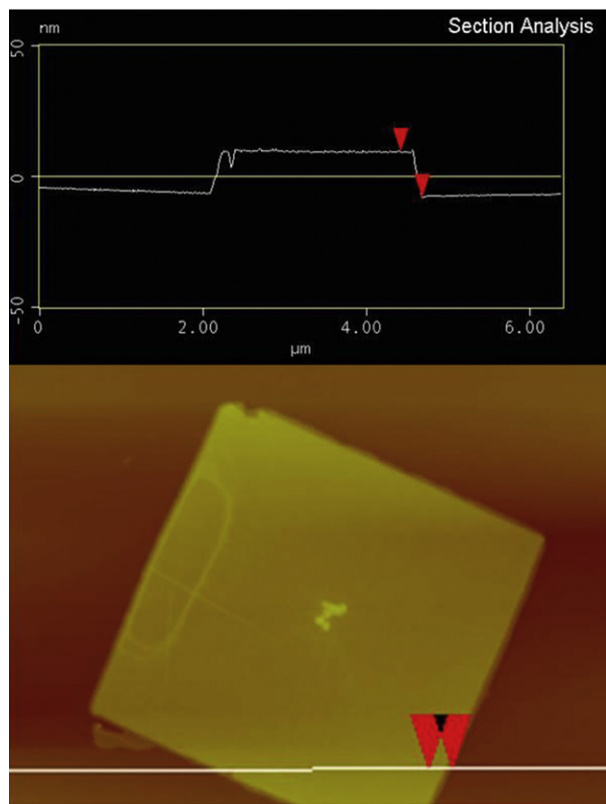[b] Polydispersity index.
[c] Weight percentage of gold.
[d] Molar ratio between PEO and PMMA.
[e] Mass ratio between PEO and PMMA.
[f] Number of polymer chain on each AuNP.
[g] grafting density (chains/nm^2).

Fig. 7. AFM images of a 5 K g/mol PEO single crystal and the corresponding height profile. The single crystal is 16 nm in thickness.

3.5. Surface plasmon resonance (SPR) study of polymer-modified Janus and symmetric AuNPs in organic solvents

AuNPs are known for SPR absorption in the visible spectrum, which reflects the collective resonance of the conducting electrons of the particle with the incident light [78,79]. Because of the influence of the ligands on the surface electron movement, surface modification of AuNPs organic ligands affects SPR of the nanoparticles [80–82]. In the present case, asymmetric modification of AuNPs with bicompartment brushes renders interesting SPR behaviors of the nanoparticles in organic solvents. Acetone was used because it is a good solvent for both PEO and PMMA. In order
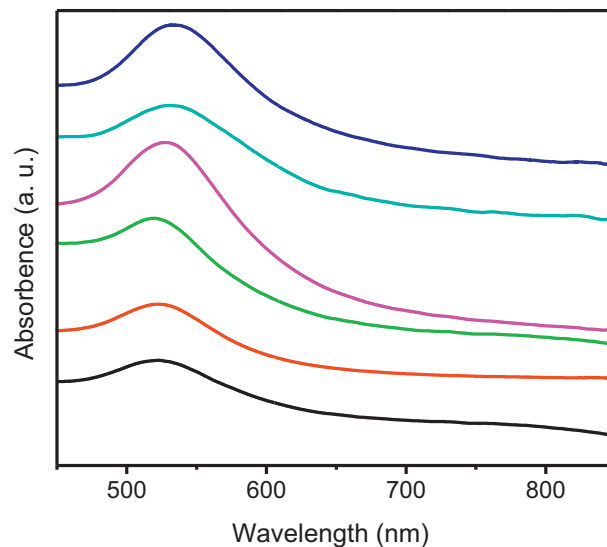
Fig. 9. UV/Vis spectra of polymer-modified AuNPs in acetone. From bottom to top: JNP PEO_{114}-Au_6-$PMMA_{118}$, PEO_{114}-Au_6-$PMMA_{138}$, PEO_{114}-Au_6-$PMMA_{208}$, symmetric AuNPs $PMMA_{130}$-Au_6, PEO_{114}/$PMMA_{152}$-Au_6, PEO_{114}/I-Au_6.

to compare the SPR adsorption of symmetric and asymmetric AuNPs, symmetric AuNPs modified with either PEO or PMMA with similar grafting densities were synthesized as described in the Experimental section. As shown in Fig. 9, the Janus AuNP modified with PEO and PMMA has a SPR band at 521–524 nm, which blue-shifted by ∼2–5 nm from that of $PMMA_{130}$-Au_6 (526 nm) and ∼10–13 nm from PEO-modified AuNPs (PEO_{114}/I-Au_6, 534 nm). According to Vilain et al. [79], this blue shift of SPR is one of the important properties of JNPs and can be attributed to the asymmetric electron-withdraw of surface ligands. The asymmetric effect on surface electrons would be averaged to zero for symmetric AuNPs, which means that the mixed-brush-modified AuNPs would show SPR band between those of homo PEO- and PMMA-modified AuNPs. To confirm this, AuNPs coated with PEO/PMMA mixed brushes were synthesized, and as shown in Fig. 9, the mix-brush-modified AuNPs has a SPR absorption band at 532 nm, which is in the center of the absorption bands of $PMMA_{130}$-Au_6 and PEO_{114}/I-Au_6. This result further confirms the asymmetric modification of AuNPs based on polymer single crystals.
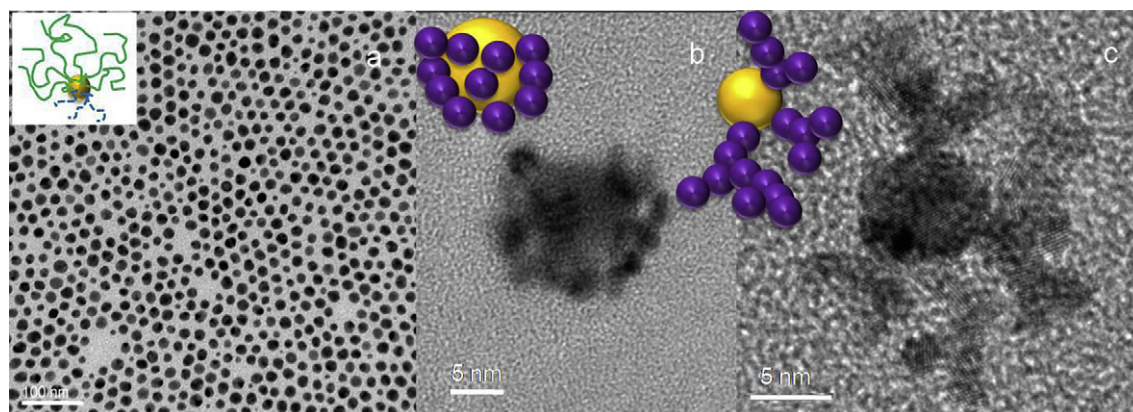
Fig. 8. TEM images of (a) PEO- and PtBA-modified Janus AuNPs on water surface, (b) PtNP-decorated Janus AuNPs with the diameter of 15 nm, and (c) PtNP-decorated Janus AuNPs with the diameter of 6 nm.

4. Conclusion

In summary, Janus AuNPs modified with bicompartment polymer brushes (PEO/PMMA, PEO/PtBA, and PEO/PAA) have been synthesized by combining polymer single crystal templating (grafting-to) and surface-initiated ATRP (grafting from) methods. The surface modification of AuNPs was confirmed using ^{1}H NMR and FTIR. The grafting density of polymer brushes was calculated using ^{1}H NMR, TGA and GPC results. PEO grafting density decreased by a factor of 2 as the polymer molecular weight increased from 2 K to 5 K g/mol. This was attributed to the decreased thiol areal density on the single crystal surface for the high molecular weight sample. The grafting density of PMMA chains also decreased with PMMA molecular weight. The Janus feature of the particles was confirmed using both PtNP decoration and UV/Vis spectroscopy analysis. In particular, the SPR adsorption band of Janus AuNPs with bicompartment polymer brushes showed a clear blue shift compared with that of symmetrical AuNPs with homo or mixed polymer brushes. Our approach demonstrated a facile way to synthesize well-defined, sub-10 nm diameter Janus nanoparticles with bicompartment polymer brushes. Structure and assembly behaviors of this novel nanoparticle will be explored in our future study.

Acknowledgment

Appendix. Supporting information

The supporting information associated with this article can be found, in the on-line version, at doi:10.1016/j.polymer.2010.08.016.

References

[1] Perro A, Reculusa S, Ravaine S, Bourgeat-Lami EB, Duguet E. J Mater Chem 2005;15(35–36):3745–60.
[2] Glotzer SC. Science 2004;306(5695):419–20.
[3] De Gennes PG. Rev Mod Phys 1992;64(3):645–8.
[4] Walther A, Muller AHE. Soft Matter 2008;4(4):663–8.
[5] Ropponen J, Nummelin S, Rissanen K. Org Lett 2004;6(15):2495–7.
[6] Percec V, Imam MR, Bera TK, Balagurusamy VSK, Peterca M, Heiney PA. Angew Chem Intern Ed 2005;44(30):4739–45.
[7] Erhardt R, Zhang MF, Boker A, Zettl H, Abetz C, Frederik P, et al. J Am Chem Soc 2003;125(11):3260–7.
[8] Voets IK, Fokkink R, Hellweg T, King SM, de Waard P, de Keizer A, et al. Soft Matter 2009;5(5):999–1005.
[9] Walther A, Andre X, Drechsler M, Abetz V, Muller AHE. J Am Chem Soc 2007;129(19):6187–98.
[10] Du YZ, Tomohiro T, Zhang G, Nakamura K, Kodaka M. Chem Commun 2004;(5):616–7.
[11] Cayre O, Paunov VN, Velev OD. J Mater Chem 2003;13(10):2445–50.
[12] Cayre O, Paunov VN, Velev OD. Chem Commun 2003;(18):2296–7.
[13] Love JC, Gates BD, Wolfe DB, Paul KE, Whitesides GM. Nano Lett 2002;2(8):891–4.
[14] Correa-Duarte MA, Salgueirino-Maceira V, Rodriguez-Gonzalez B, Liz-Marzan LM, Kosiorek A, Kandulski W, et al. Adv Mater 2005;17(16):2014–8.
[15] Hugonnot E, Carles A, Delville MH, Panizza P, Delville JP. Langmuir 2003;19(2):226–9.
[16] Velev OD, Lenhoff AM, Kaler EW. Science 2000;287(5461):2240–3.
[17] Fujimoto K, Nakahama K, Shidara M, Kawaguchi H. Langmuir 1999;15(13):4630–5.
[18] Srivastava Y, Marquez M, Thorsen T. Biomicrofluidics 2009;3:012801–6.
[19] Suzuki D, Tsuji S, Kawaguchi H. J Am Chem Soc 2007;129(26):8088–9.
[20] Schmid G, Simon U. Chem Commun 2005;(6):697–710.
[21] Manoharan VN, Elsesser MT, Pine DJ. Science 2003;301(5632):483–7.
[22] Roh KH, Yoshida M, Lahann J. Langmuir 2007;23(10):5683–8.
[23] Mathiowitz E, Jacob JS, Jong YS, Carino GP, Chickering DE, Chaturvedi P, et al. Nature 1997;386(6623):410–4.
[24] Choi J, Zhao YH, Zhang DY, Chien S, Lo YH. Nano Lett 2003;3(8):995–1000.
[25] Nie L, Liu SY, Shen WM, Chen DY, Jiang M. Angew Chem Intern Ed 2007;46(33):6321–4.
[26] Walther A, Hoffmann M, Muller AHE. Angew Chem Intern Ed 2008;47(4):711–4.
[27] van Herrikhuyzen J, Portale G, Gielen JC, Christianen PCM, Sommerdijk N, Meskers SCJ, et al. Chem Commun 2008;(6):697–9.
[28] Kang YJ, Erickson KJ, Taton TA. J Am Chem Soc 2005;127(40):13800–1.
[29] Srivastava S, Kotov NA. Soft Matter 2009;5(6):1146–56.
[30] Crossley S, Faria J, Shen M, Resasco DE. Science 2010;327:68–72.
[31] McConnell MD, Kraeutler MJ, Yang S, Composto RJ. Nano Lett 2010;10(2):603–9.
[32] Wang DY, Mohwald H. J Mater Chem 2004;14(4):459–68.
[33] Yin YD, Lu Y, Xia YN. J Am Chem Soc 2001;123(4):771–2.
[34] Giersig M, Ung T, LizMarzan LM, Mulvaney P. Adv Mater 1997;9(7):570–5.
[35] Gu HW, Zheng RK, Zhang XX, Xu B. J Am Chem Soc 2004;126(18):5664–5.
[36] Higuchi T, Tajima A, Yabu H, Shimomura M. Soft Matter 2008;4(6):1302–5.
[37] Teranishi T, Inoue Y, Nakaya M, Oumi Y, Sano T. J Am Chem Soc 2004;126(32):9914–5.
[38] Yu H, Chen M, Rice PM, Wang SX, White RL, Sun SH. Nano Lett 2005;5(2):379–82.
[39] Reculusa S, Poncet-Legrand C, Ravaine S, Mingotaud C, Duguet E, Bourgeat-Lami E. Chem Mater 2002;14(5):2354–9.
[40] Yake AM, Panella RA, Snyder CE, Velegol D. Langmuir 2006;22(22):9135–41.
[41] Paunov VN, Cayre OJ. Adv Mater 2004;16:788–91.
[42] Takei H, Shimizu N. Langmuir 1997;13(7):1865–8.
[43] Lu Y, Xiong H, Jiang XC, Xia YN, Prentiss M, Whitesides GM. J Am Chem Soc 2003;125(42):12724–5.
[44] Petit L, Sellier E, Duguet E, Ravaine S, Mingotaud C. J Mater Chem 2000;10(2):253–4.
[45] Gu HW, Yang ZM, Gao JH, Chang CK, Xu B. J Am Chem Soc 2005;127(1):34–5.
[46] Glaser N, Adams DJ, Boker A, Krausch G. Langmuir 2006;22(12):5227–9.
[47] Boker A, He J, Emrick T, Russell TP. Soft Matter 2007;3:1231–48.
[48] Maye MM, Nykypanchuk D, Cuisinier M, van der Lelie D, Gang O. Nat Mater 2009;8(5):388–91.
[49] Loweth CJ, Caldwell WB, Peng XG, Alivisatos AP, Schultz PG. Angew Chem Intern Ed 1999;38(12):1808–12.
[50] Xu XY, Rosi NL, Wang YH, Huo FW, Mirkin CA. J Am Chem Soc 2006;128(29):9286–7.
[51] Hong L, Jiang S, Granick S. Langmuir 2006;22(23):9495–9.
[52] DeVries GA, Brunnbauer M, Hu Y, Jackson AM, Long B, Neltner BT, et al. Science 2007;315(5810):358–61.
[53] Kim BJ, Bang J, Hawker CJ, Chiu JJ, Pine DJ, Jang SG, et al. Langmuir 2007;23(25):12693–703.
[54] Lattuada M, Hatton TA. J Am Chem Soc 2007;129:12878–89.
[55] Li B, Li CY. J Am Chem Soc 2007;129(1):12–3.
[56] Li B, Ni C, Li CY. Macromolecules 2008;41(1):149–55.
[57] Wang BB, Li B, Zhao B, Li CY. J Am Chem Soc 2008;130(35):11594–5.
[58] Geil P. Polymer single crystals. Huntington, N.Y.: Robert Krieger Pub.; 1973.
[59] Li CY. J Poly Sci Poly Phys 2009;47:2436–40.
[60] Chen WY, Li CY, Zheng JX, Huang P, Zhu L, Ge Q, et al. Macromolecules 2004;37(14):5292–9.
[61] Chen WY, Zheng JX, Cheng SZD, Li CY, Huang P, Zhu L, et al. Phys Rev Lett 2004;93(2):028301–4.
[62] Li L, Li B, Hood MA, Li CY. Polymer 2009;50(4):953–65.
[63] Li LY, Li CY, Ni CY. J Am Chem Soc 2006;128(5):1692–9.
[64] Li B, Li LY, Wang BB, Li CY. Nat Nanotech 2009;4(6):358–62.
[65] Wang BB, Li B, Xiong J, Li CY. Macromolecules 2008;41(24):9516–21.
[66] Li B, Wang BB, Ferrier RCM, Li CY. Macromolecules 2009;42(24):9394–9.
[67] Wang B, Li B, Ferrier RCM, Li CY. Macromol Rapid Commun 2010;31:169–75.
[68] Barbey R, Lavanant L, Paripovic D, Schüwer N, Sugnaux C, Tugulu Sa, et al. Chem Rev 2009;109:5437–527.
[69] Zhao B, Zhu L. Macromolecules 2009;42(24):9369–83.
[70] Jana NR, Peng XG. J Am Chem Soc 2003;125(47):14280–1.
[71] Control experiments have been carried out under the same condition at the absence of PEO114-Au6-I to study the influence of initiator **1** on possible disulfide bond formation of PMMA chains prepared by ATRP. After polymerization, tributylphosphine (Bu3P) was used to cleave possible disulfide bonds. Our results showed that the molecular weights of PMMA prepared by ATRP before and after Bu3P treatment remained the same, indicating that disulfide bonds were not formed.
[72] Worden JG, Shaffer AW, Huo Q. Chem Commun 2004;(5):518–9.
[73] Xia JH, Gaynor SG, Matyjaszewski K. Macromolecules 1998;31(17):5958–9.
[74] Kim JB, Bruening ML, Baker GL. J Am Chem Soc 2000;122(31):7616–7.
[75] Shaffer AW, Worden JG, Huo Q. Langmuir 2004;20(19):8343–51.
[76] Templeton AC, Hostetler MJ, Kraft CT, Murray RW. J Am Chem Soc 1998;120(8):1906–11.
[77] Ohno K, Morinaga T, Koh K, Tsujii Y, Fukuda T. Macromolecules 2005;38(6):2137–42.
[78] Kreibig U, Genzel L. Surf Sci Jun 1985;156:678–700.
[79] Vilain C, Goettmann F, Moores A, Le Floch P, Sanchez C. J Mater Chem 2007;17(33):3509–14.
[80] Haes AJ, Zou SL, Schatz GC, Van Duyne RP. J Phys Chem B 2004;108:6961–8.
[81] Noguez CJ. Phys Chem C 2007;111(10):3806–19.
[82] Hodes G. Adv Mater 2007;19(5):639–55.